FETCH AND FOOTPRINT OF TURBULENT FLUXES OVER VEGETATIVE STANDS WITH ELEVATED SOURCES

XUHUI LEE*
School of Forestry and Environmental Studies, Yale University, 370 Prospect Street, New Haven, CT 06511, U.S.A.

(Received in final form 30 July 2002)

Abstract. In this study, Raupach's localized near-field (LNF) theory is combined with appropriate parameterizations of the turbulence inside a canopy to investigate how air stability and source configuration influence the flux footprint and flux adjustment with fetch in the roughness sublayer. The model equations are solved numerically. The flux footprint from the LNF prediction is in general more contracted than the prediction based on the inertial sublayer similarity functions. In very unstable conditions, the near-field effect causes the footprint of the elevated canopy source to locate further upwind than that of the ground-level source, and the combined footprint can become negative in situations where the two sources are of opposite sign. The flux footprint and flux adjustment with fetch in the roughness sublayer are sensitive to source configuration and the parameters specifying wind speed and the Lagrangian time scale inside the canopy.

Keywords: Canopy turbulence, Fetch, Footprint.

1. Introduction

In micrometeorology, footprint theory is widely used for the interpretation of the vertical scalar flux in the atmospheric surface layer. A number of models of flux footprint and flux adjustment with fetch are built upon the principles of gradient-diffusion established for relatively smooth surfaces. The applicability of these models in the roughness sublayer over a vegetation canopy is questionable because the scalar exchange in the roughness sublayer is influenced by dual-source diffusion resulting from the elevated canopy source and the ground-level source. It is known that the conventional gradient-diffusion theory is inadequate for describing the diffusion processes of a spatially distributed source. Furthermore, turbulent transport is dominated by the coherent eddies that are generated by shear instability linked to the inflected wind profile near the top of the canopy layer, whereas in the smooth-wall surface layer the wind profile does not possess such an inflection point. A consequence of the shear-instability is that eddy diffusivity for scalar constituents is enhanced over that predicted by the Monin–Obukhov similarity theory. Such enhancement would cause the footprint to locate closer to the observational point than a prediction based only on the surface-layer similarity functions. Fi-

* E-mail: xuhui.lee@yale.edu

Boundary-Layer Meteorology **107:** 561–579, 2003.

nally, because wind speed does not diminish at the source height, the emission plume will advect further downwind before it is detected by a flux instrument, thus counter-acting the effect of the enhanced eddy diffusion in the roughness sublayer.

In this study, we use a model (Model I) that combines the localized near-field (LNF) theory of Raupach (1989) with appropriate parameterizations of the turbulence in the canopy to investigate the adjustment of the vertical eddy flux with fetch in the roughness sublayer. The results of the model calculations will be compared with predictions from a second model (Model II) that uses only the inertial sublayer similarity functions to determine the sensitivity of the flux footprint calculation to the canopy turbulence formulation. The model equations are solved numerically, using the method of Patankar (1980). An advantage of the numerical approach is that it is free of some of the simplifications required to achieve an analytical solution, which is sought by some published studies on flux adjustment (see a recent review by Schmid, 2002). Thus, like stochastic Lagrangian simulations and the large-eddy simulation technique (Leclerc and Thurtell, 1990; Horst and Weil, 1992; Wilson and Swaters, 1991; Leclerc et al., 1997), the numerical approach should improve the physical realism represented by the analytical models. It is true that the numerical approach is computationally less efficient than an analytical one. However, this is no longer a serious limitation given the computing power offered by today's desktop computers.

2. Model I: Model with an Elevated Source

2.1. Basic equations

This section develops equations for a model (Model I) that incorporates the LNF theory and the canopy turbulence formulation. In the LNF theory, the scalar concentration resulting from the canopy source is separated into a non-diffusive near-field and a diffusive far-field component. The dominance of the coherent eddy transport is represented by a large Lagrangian time scale that is invariant with height in the upper canopy layer and in the roughness sublayer. Baldocchi (1997) adopted the LNF parameterization of the Lagrangian time scale in his random flight simulation of flux footprint for the ground-level source inside forests.

Let a step change from zero to F_T in the total net ecosystem exchange (NEE) occur at the leading edge ($x = 0$) and let F_T be partitioned as

$$F_T = F_e + F_g, \tag{1}$$

where F_e and F_g are strengths of the elevated and the ground-level sources, respectively. The far-field concentration field, c_F, which is contributed by both sources, is diffusive, and follows the diffusion equation

$$F = -K_F \frac{\partial c_F}{\partial z}, \tag{2}$$

and the conservation equation

$$u\frac{\partial c_F}{\partial x} + \frac{\partial F}{\partial z} = s^*, \tag{3}$$

where F is the vertical flux, z is height above the ground, u is horizontal velocity, x is horizontal distance from the leading edge, and s^* is a source term. The far-field eddy diffusivity, K_F, is given by

$$K_F = \sigma_w^2 \tau, \tag{4}$$

where σ_w is the standard deviation of the vertical velocity and τ is a Lagrangian time scale. To be consistent with most models of flux adjustment with fetch, the divergence of the streamwise eddy flux is ignored here. Baldocchi (1997), Rannik et al. (2000) and Lee (2002) show that this simplification may distort the flux footprint near the observational point but does not alter the broad pattern of flux adjustment with fetch.

The non-diffusive, near-field concentration, which is contributed by the elevated source only, is transported by the mean wind. To conserve mass, Raupach (1989) proposes the following relationship between the source term s^* and the real source density, s

$$s^* = \begin{cases} 0 & \text{for } x \le u\tau \\ s & \text{for } x > u\tau \end{cases}. \tag{5}$$

A comparison by Warland and Thurtell (2000) with a Lagrangian solution to the within-canopy concentration profile suggests that LNF underestimates the near-field effect near the top of the canopy. It is possible that the principles established by these authors can further improve the physics of the footprint simulation.

The boundary conditions are

$$\left.\begin{array}{ll} c_F = 0, & x = 0 \\ F = F_g, & z = 0 \\ \dfrac{\partial c_F}{\partial z} = 0, & z = 40h \end{array}\right\} \tag{6}$$

where h is canopy height

The flux footprint, f, is computed from

$$f = \frac{1}{F_T}\frac{\partial F}{\partial x}. \tag{7}$$

Horst and Weil (1994) showed that, for a ground-level source, S, in a horizontally homogeneous flow, f from Equation (7) is equivalent to the conventional definition of a footprint function such that

$$F(x, z) = \int_0^\infty S(x - x')\, f(x', z)\mathrm{d}x'. \tag{8}$$

In the case of a vertically distributed source, the principle of superposition leads to

$$F(x,z) = \sum_{i=1}^{n} \int_0^{\infty} F_i(x'-x)\, f_i(x',z)\mathrm{d}\,x', \tag{9}$$

where F_i is the source strength of layer i, and f_i is the footprint function for this layer. For a horizontally uniform source with a step change at $x = 0$ and in horizontally homogeneous flow, substitution of Equation (9) into Equation (7) gives

$$f = \sum_{i=1}^{n} \frac{F_i}{F_T} f_i. \tag{10}$$

Thus, f represents a combined footprint function that is a source strength-weighted average of the footprints of individual layers. Equation (7) offers a convenient way of determining the combined footprint. Alternatively, one can first determine the flux footprint for each layer by replacing the continuous source distribution function (Equation (16) below) with discrete layers and setting the source strength of all other layers to zero, and then calculate the combined footprint from Equation (10). Because of the principle of superposition, the combined footprint can become negative if one or more of the layers have a source strength that is opposite in sign to NEE (Section 4).

2.2. Parameterizations

The mean wind profile in the air layer over the canopy is given by

$$\frac{u}{u_*} = \frac{1}{k}\left\{\ln\frac{z-d}{z_o} - \Psi_m(\frac{z-d}{L}).\right\}, \tag{11}$$

where L is the Obukhov length, d is displacement height, z_o is surface roughness length, u_* is friction velocity, k (= 0.4) is the von Karman constant, and Ψ_m is a stability correction factor

$$\Psi_m(y) = \begin{cases} \ln\left\{\left(\dfrac{1+\eta^2}{2}\right)\left(\dfrac{1+\eta}{2}\right)^2\right\} - 2\arctan\eta + \dfrac{\pi}{2} & \text{for } y \le 0 \\ -5y & \text{for } y > 0 \end{cases} \tag{12}$$

with $\eta = (1-16y)^{1/4}$. The two aerodynamic parameters are specified as $d/h = 0.6$ and $z_o/h = 0.1$. Equation (11), even though based on the similarity relationships for the smooth-wall surface layer, predicts the stability dependence of u/u_* that agrees with observations over a wide height and stability ranges over forests (Figure 1). To obtain wind speed inside the canopy, we use

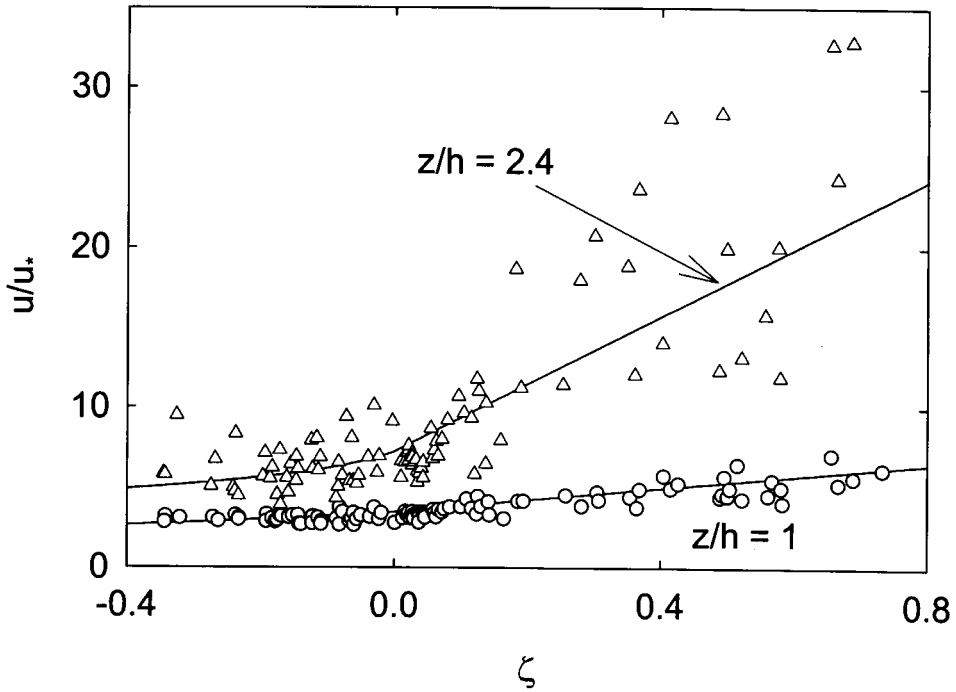

Figure 1. Nondimensional wind speed as a function of air stability. Solid lines represent Equation (11) and symbols are observations by Shaw et al. (1988) at the Borden forest.

$$u = u_h \left\{ \frac{\sinh(\alpha z/h)}{\sinh(\alpha)} \right\}^{1/2}, \tag{13}$$

where wind speed at the canopy top, u_h, is given by Equation (11) for $z = h$. Equation (13) is chosen over the exponential model because it captures both the exponential behavior in the upper canopy layer and the logarithmic pattern near the ground. Parameter α takes a value of 6.5, which provides the best match between Equation (13) and the observed profile in the Borden forest (Shaw et al., 1988) and the profile simulated with a second-order closure model for a canopy with a leaf area index of 4 (Lee et al., 1994). The profile of u (as well as those of σ_w, τ and K_F) is not a smooth function of z; this does not present any difficulty for the numerical scheme used in the present study. However, for the inverse problem, smooth profiles are highly desirable (Leuning, 2000; Katul et al., 2001).

The vertical velocity standard deviation over the canopy is given by

$$\frac{\sigma_w}{u_*} = \begin{cases} 1.25(1 - 3\dfrac{z-d}{L})^{1/3} & \text{for } L \le 0 \\ 1.25 & \text{for } L > 0 \end{cases}. \tag{14}$$

Equation (14) has also been confirmed over a wide variety of vegetated stands (e.g., Ohtaki, 1985; Raupach et al., 1986). The profile of σ_w inside the canopy is specified as

$$\frac{\sigma_w}{u_*} = \frac{\sigma_{w,h}}{u_*}[(1 - a_o)\frac{z}{h} + a_o], \tag{15}$$

where $\sigma_{w,h}$, the vertical velocity standard deviation at the canopy top, is given by Equation (14) for $z = h$. The default a_o value is 0.2.

The elevated (canopy) source density is a function of height only, and is distributed according to

$$s = \frac{F_e}{h}\frac{1}{0.125\sqrt{2\pi}}\exp[-(z/h - 0.65)^2/(2 \times 0.125^2)]. \tag{16}$$

The Gaussian profile, which is often used in canopy flow models to approximate the vertical leaf area distribution of the overstory, satisfies the requirement $F_e = \int_0^h s\mathrm{d}z$.

The τ profile is specified as (Kaimal and Finnigan, 1994)

$$\tau = \begin{cases} K/\sigma_w^2 & \text{for } z > z_r \\ \beta & \text{for } 0.25h < z \le z_r \\ \beta z/(0.25h) & \text{for } z \le 0.25h, \end{cases} \tag{17}$$

where K is the eddy diffusivity of the inertial sublayer from

$$K = ku_*(z - d)/\phi_c[(z - d)/L], \tag{18}$$

and z_r, the vertical extent of the roughness sublayer, is set to $2.16h$. This value is chosen so that the normalized Lagrangian time scale takes the recommenced value in the roughness sublayer for neutral air. The stability function, ϕ_c, is given by

$$\phi_c(y) = \begin{cases} (1 - 16y)^{-1/2} & \text{for } y \le 0 \\ (1 + 5y) & \text{for } y > 0. \end{cases} \tag{19}$$

The exact form of β, the Lagrangian time scale in the upper canopy and in the roughness sublayer, is poorly known. In the absence of theoretical and experimental guidelines, Leuning (2000) proposed a stability corrected β by matching the far-field eddy diffusivity with its inertial sublayer limit. Thus

$$\beta = k(z_r - d)/\left\{u_*\phi_c(\frac{z_r - d}{h}\zeta)[\phi_w(\frac{z_r - d}{h}\zeta)]^2\right\}, \tag{20}$$

where ζ is a stability parameter defined as $\zeta = h/L$. The nondimensional Lagrangian time scale, $\beta u_*/h$, is a function of ζ. It takes a value of 0.64 at $\zeta = -1$

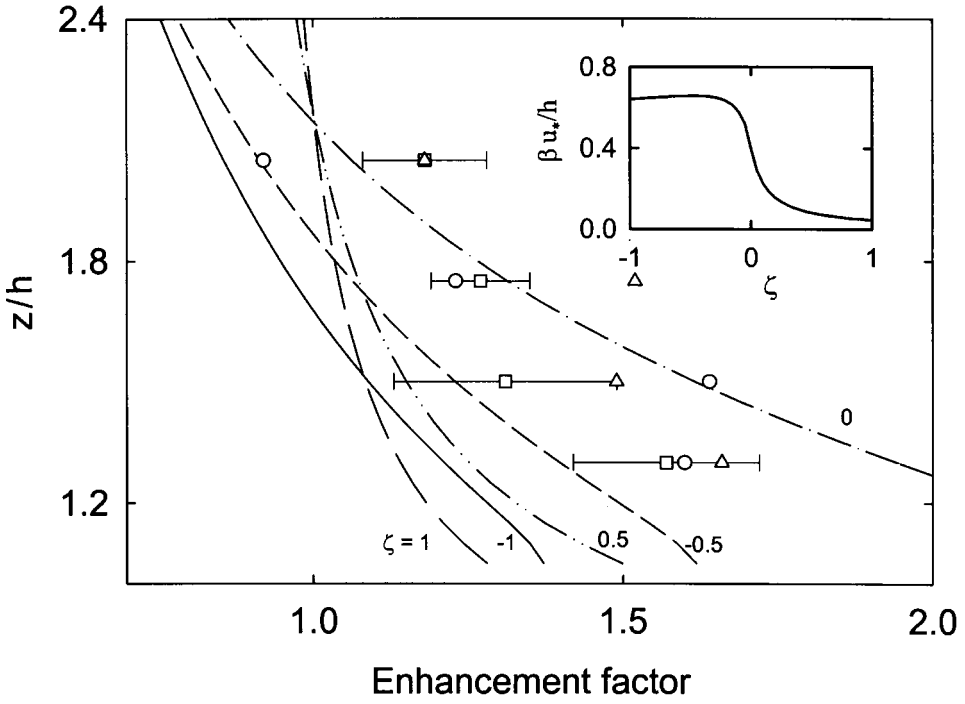

Figure 2. Eddy diffusivity enhancement factor calculated from the LNF theory using the stability-dependent Lagrangian time scale in the canopy layer and in the roughness sublayer (insert). Data points are the average enhancement factor observed by Simpson et al. (1998) over the Borden forest before leaf senescence (circles, unstable conditions; squares, neutral; triangles, stable; error bars, ± 1 standard deviation).

and 0.40 at $\zeta = 0$, the latter of which is the value recommenced for neutral air (Leuning, 2000), and decreases to 0.05 at $\zeta = 1$ (Figure 2 inset).

Leuning (2000) found that once the stability correction on the Lagrangian time scale was accounted for by Equation (20), excellent agreement was obtained between the observed fluxes of heat, water vapor and carbon dioxide over a rice paddy and predictions from the inverse LNF analysis. Baldocchi and Harley (1995) computed their Lagrangian dispersion matrix as a function of air stability. Another way of checking the validity of Equation (20) is to compare the eddy diffusivity enhancement observed in the roughness sublayer with the prediction from the LNF theory. To do this, we first compute the total concentration, C (the sum of the far- and near-field components), from the LNF theory using the Lagrangian time scale (Equation (20)) and the profiles of σ_w and s (Equations (14)–(16)) for a given stability condition. An apparent eddy diffusivity is first computed from $K_a = -F_T/(\partial C/\partial z)$ and then divided by the inertial sublayer diffusivity (Equation (18)) to produce a vertical profile of the eddy diffusivity enhancement factor, K_a/K. A comparison with the observation by Simpson et al. (1998) for the Borden forest is given in Figure 2. Simpson et al. (1998) show that the eddy diffusivity

enhancement factor has a maximum value near the treetops and decreases with increasing height. The result from the LNF theory agrees reasonably well with their observation.

2.3. Numerical method

Before a numerical solution of the model equations is sought, all the variables are made nondimensional by u_*, h, F_T, thus eliminating the dependence of the solution on these three scaling variables. The model equations are discretized according to Patankar (1980), with an upwind scheme for the advection term of Equation (3). The vertical grid size is 0.05 $(z_m - d)$, and the horizontal grid size is 0.05 $(z_m - d)$ for $x \leq 5h$ and 0.2 $(z_m - d)$ for $x > 5h$, where z_m is measurement height. The solution for c_F is sought with a line-by-line method in the forward wind direction, until the vertical flux at the height of z_m reaches a pre-specified value. The flux footprint is then computed from Equation (7).

3. Model II: Model Using the Surface-Layer Functions Only

In the same spirit as Rannik et al. (2000), a second model (Model II) is used in conjunction with the above model to investigate the influence of canopy turbulence formulation on the calculation of flux adjustment and also to allow comparisons with the published models. This model consists of Equation (7), the wind and eddy diffusivity profiles (Equations (11) and (18)), and the following equations

$$F = -K\frac{\partial c}{\partial z} \tag{21}$$

$$u\frac{\partial c}{\partial x} + \frac{\partial F}{\partial z} = 0. \tag{22}$$

The boundary conditions are

$$\left.\begin{array}{ll} c = 0, & x = 0 \\ F = F_T, & z - d = 0 \\ \dfrac{\partial c_F}{\partial z} = 0, & z - d = 40(z_m - d) \end{array}\right\} \tag{23}$$

Equations (21)–(23) imply (a) that all the sources are located at height $z = d$, (b) that there is no near-field contribution to the concentration field, and (c) that there is no roughness sublayer over the canopy. The same numerical procedure is used to solve the model equations. Once again, all variables are made nondimensional by u_*, F_T and the length scale, $z_m - d$, prior to the model computation.

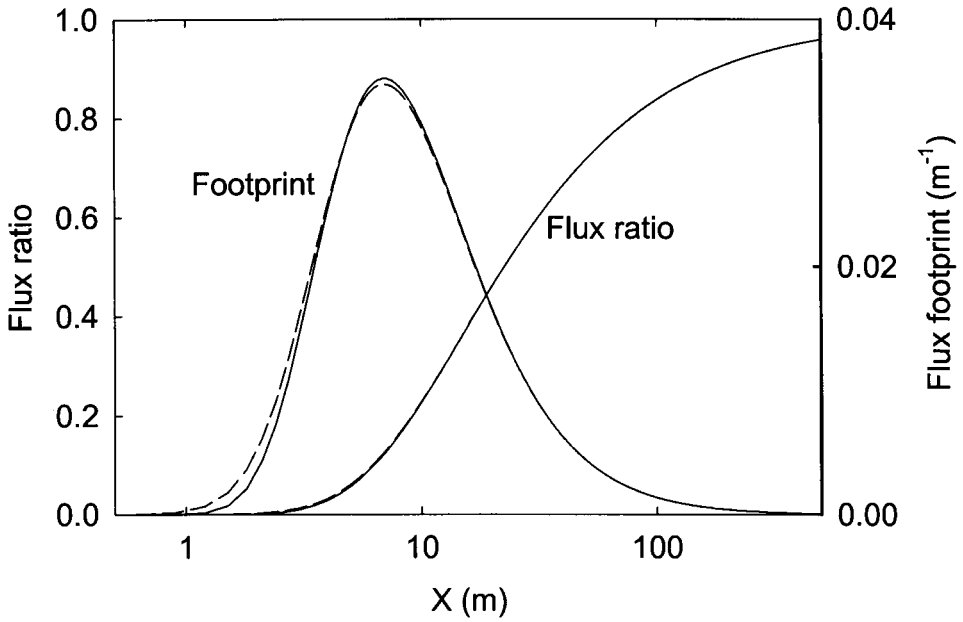

Figure 3. Comparison of the numerical calculation (dashed lines) with Philip's (1959) analytical solution (solid lines) of flux adjustment and footprint function at the height of 1 m above the ground.

4. Results and Discussion

4.1. Comparison with analytical solutions

Philip (1959) derived an exact solution to Equations (21)–(23) using power functions for the wind and eddy diffusivity profiles. His solution was later deployed by Dyer (1963) to examine flux adjustment with fetch. To check the accuracy of the numerical procedure, we replace Equation (11) and (18) with those given by Dyer (1963) and compare the numerical solution of Model II with the analytical one (Figure 3). The numerical procedure gives the vertical flux and flux footprint that are virtually indistinguishable from the exact solution except a slight overestimation of the footprint distribution near the observational point. Therefore, the accuracy of the numerical solution for the flux distribution is adequate for most practical purposes.

Figure 4 compares the results from Model II and the analytical model of Horst and Weil (1994) for two $(z_m - d)/z_o$ ratios. The two models agree reasonably well in terms of the overall shape and magnitude of the footprint function (Figure 4a) and the stability dependence of fetch requirement (Figure 4b), but differ in several details. First, Model II predicts a footprint peak closer to the observational point. Second, its peak value is slightly lower for the smooth surface and slightly higher for the rough surface than Horst and Weil's model prediction, although the latter is probably not intended for very rough surfaces because their solutions were

established from diffusion experiments over surfaces with short vegetation. Finally, according to Model II, it takes a longer fetch for the vertical flux to reach 80% or a higher fraction of the total NEE under unstable conditions.

4.2. FOOTPRINTS OF GROUND-LEVEL SOURCE VERSUS ELEVATED SOURCE

Figure 5 compares footprints of the ground-level and elevated sources computed from Model I by setting $F_g/F_T = 1$ and $F_e/F_T = 1$, respectively. The measurement height is $1.6h$. The footprint peak shifts progressively further upwind with increasing stability for both sources as eddy diffusion is weakened under increasing stability. The two footprints are similar at near-neutral stability, but differ in stratified air. In stable air, the footprint of the ground-level source peaks further upwind than that of the elevated source, and vise versa in unstable air. The largest relative difference is found under very unstable conditions ($\zeta = -1$), which can be explained by the large near-field effect due to the large Lagrangian time scale (Figure 2 insert) that causes the footprint of the elevated source to locate further upwind. This is in spite of the fact that there is a large vertical separation between the ground-level source and the measurement height. On the other hand, the near-field effect is negligibly small in stable conditions, and the large vertical separation causes the footprint of the ground-level source to shift upwind of that of the elevated source. The footprint mismatch in unstable conditions is not a serious problem for observational studies as long as the two sources are uniform within these short fetch distances. On the contrary, the very extensive footprints and the mismatch in their peak position under stable conditions are two factors contributing to the difficulty in the interpretation of nighttime eddy fluxes.

At $\zeta = -1$, both footprints are very localized: The fetch distance for 90% flux adjustment at height $z/h = 1.6$ is 5.18 and 5.47 for the ground-level and the elevated sources, respectively. The very localized footprint under unstable conditions is also simulated by all other valid footprint models.

In Figure 6, the footprint distribution predicted by the random walk model of Baldocchi (1997) is plotted together with the prediction from Model I for the ground-level source at neutral stability. The footprint of the present study peaks at a higher value, at a position much closer to the observational point, than the random walk model. The difference arises in large part from the ways in which the physics of the canopy turbulence is parameterized. In the random walk model, the wind profile inside the canopy takes an exponential form that does not diminish at the ground, and the Lagrangian time scale is given a smaller value below height z_r hence resulting in a smaller eddy diffusivity in the canopy and in the roughness sublayer. In other words, the random walk model is more advective and less diffusive than the present model. If the default u and τ parameterizations are replaced with those used in the random walk model, a closer agreement is produced in terms of the footprint peak value and position, although some difference still remains. The high sensitivity of the model results to the turbulence parameterization and

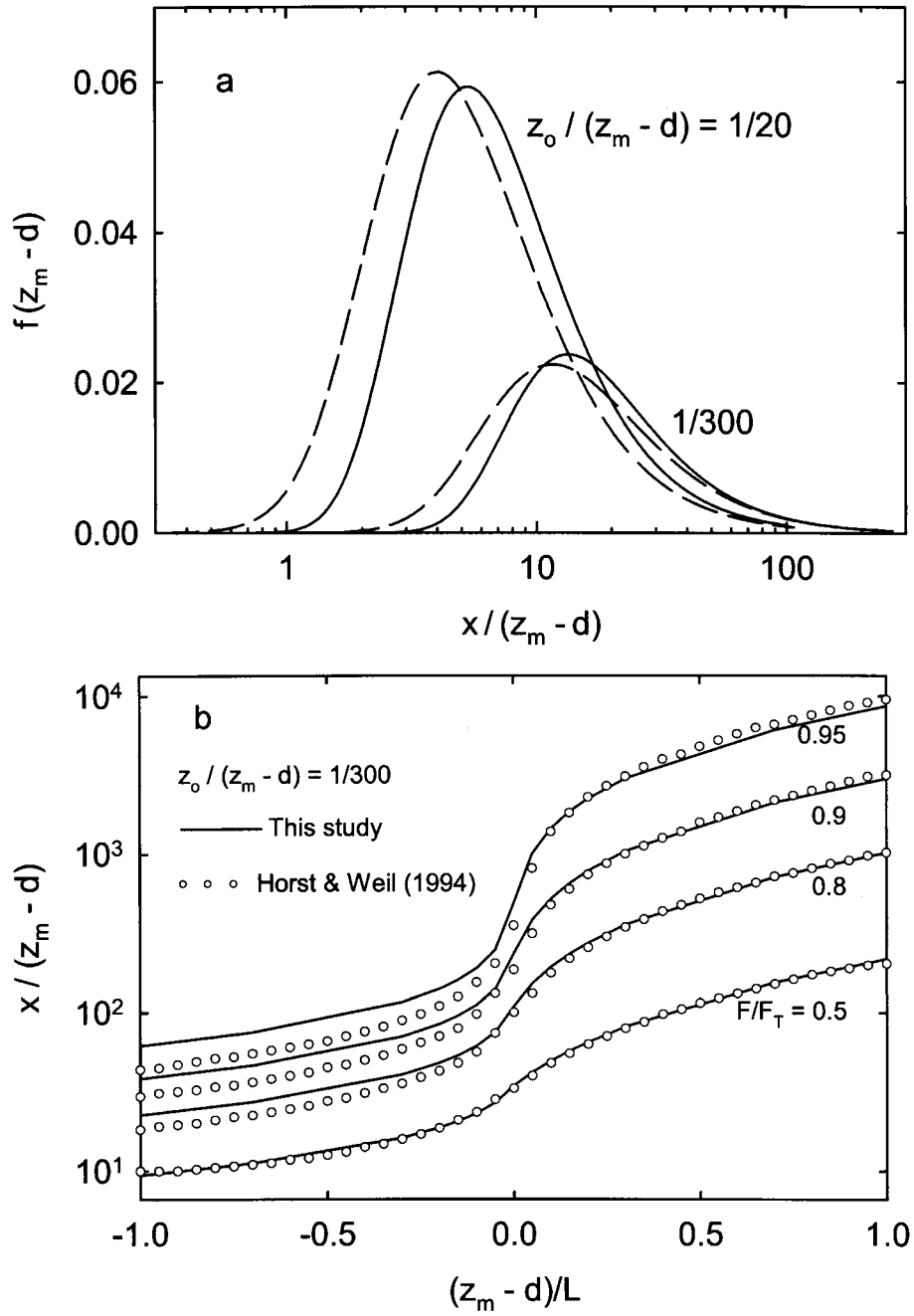

Figure 4. Comparison of calculations from Model II with the analytical results given by Horst and Weil (1994): (a) Normalized footprint function for two ratios of $(z_m - d)/z_o$ at neutral stability (solid lines, Horst and Weil; dashed lines, this study); (b) fetch distance, normalized by measurement height, as a function of air stability. Fetch distance refers to the horizontal position at which the vertical flux ratio F/F_T reaches the value specified.

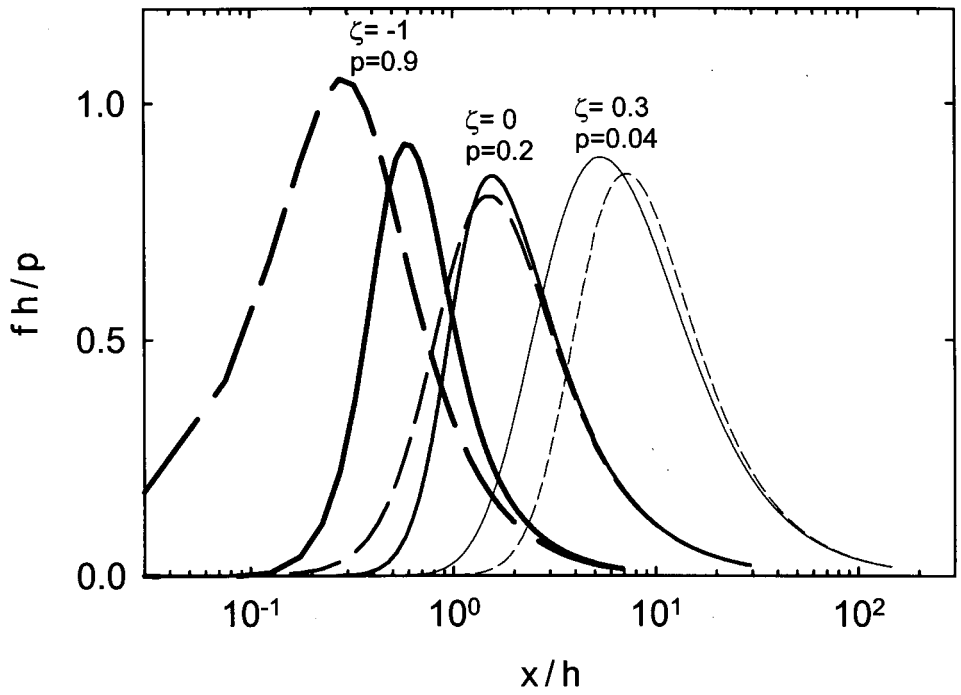

Figure 5. Normalized flux footprints of the elevated source (solid lines) and the ground-level source (dashed lines) at height z/h = 1.6 and in three stability conditions. For convenience of comparison, the footprint function is scaled by a factor p.

numerical schemes (Lagrangian versus numerical solution) highlights the need for field validation of the model predictions.

4.3. Influence of source configuration on flux footprint and fetch

Figures 7–9 present the results of the calculations made for three source configurations: $F_e/F_T = 0.8$ or $F_g/F_T = 0.2$ (configuration A), $F_e/F_T = 1.2$ or $F_g/F_T = -0.2$ (B), and $F_e/F_T = 0.2$ or $F_g/F_T = 0.8$ (C). Configuration A, in which the elevated and the ground-level sources are of the same sign and with the former dominating, is a good representation of water vapour and sensible heat exchanges in a moderately dense vegetation stand. Configuration B can be regarded as a model for carbon dioxide in the growing season in daylight hours when the elevated canopy and the ground-level sources are of opposite sign. Nighttime CO_2 exchange in a forest during the growing season and water vapour and sensible heat exchanges in a deciduous forest in the dormant season are two examples of configuration C, in which the ground-level source is the dominant one. These figures bring out several points:

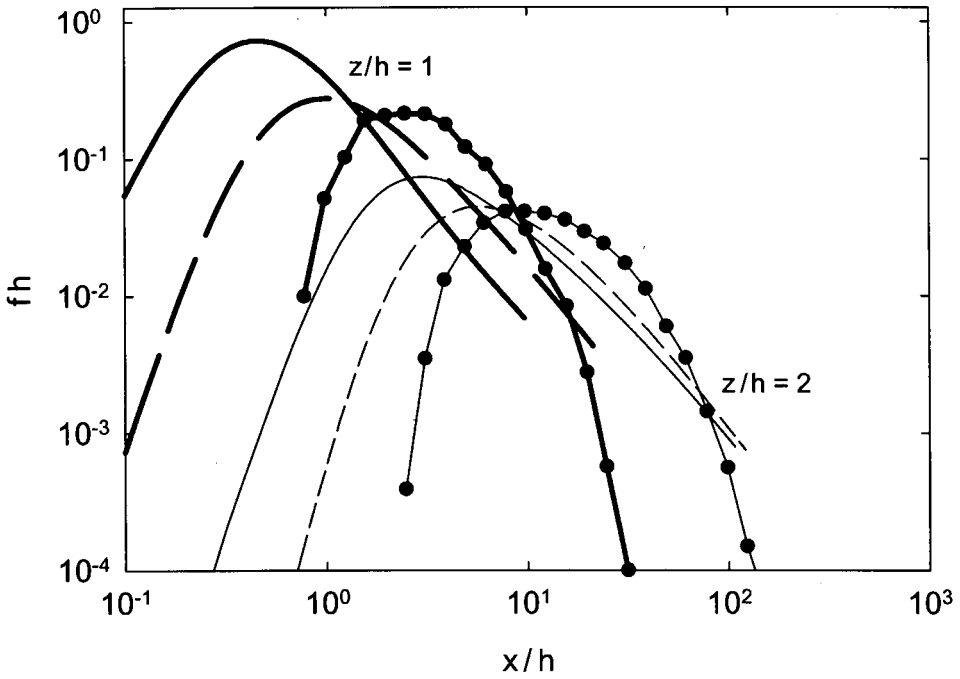

Figure 6. Comparison of the normalized flux footprint calculated from Model I and the Lagrangian simulation results found in Baldocchi (1997) for the ground-level source ($F_g/F_T = 1$) at neutral air stability: Dots, Baldocchi's results; solid lines, output from Model I with the default wind speed and Lagrangian time scale profiles; dashed lines, output from Model I using the profiles in Baldocchi (1997).

Footprints in the roughness sublayer. Footprints in the roughness sublayer are sensitive to the source distribution. In situations where NEE is dominated by the elevated source, the footprint peak is found further upwind in unstable air and closer to the observational point in stable air, than in situations where NEE is dominated by the ground-level source, consistent with the result in Figure 5. The footprint distribution becomes more contracted as the contribution of the elevated source to the total NEE increases. A negative footprint is possible in unstable air if the two sources are of opposite sign. As explained in Section 2.1, a negative combined footprint can result from a vertically distributed source and is not a mathematical artifact.

Footprints in the inertial sublayer. Once in the inertial sublayer, the influence of source configuration on the footprint is detectable only in very unstable conditions, due primarily to the large near-field effect noted above. Even then, the detectable influence is limited to roughly $0.3h$ distance upwind of the observational point (Figure 7 top panels).

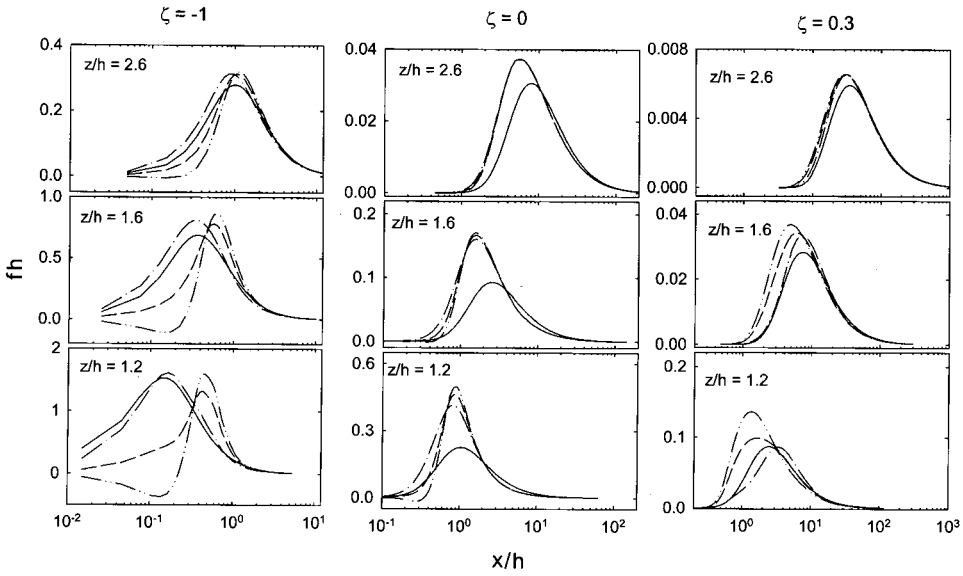

Figure 7. Normalized flux footprints at two heights within the roughness sublayer (z/h = 1.2 and 1.6) and at one height in the inertial sublayer (z/h = 2.6): Dashed line, F_e/F_T = 0.8 (configuration A); dash–dot–dot line, F_e/F_T = 1.2 (configuration B); dash–dot line, F_e/F_T = 0.2 (configuration C); solid line, calculation with Model II using $d/h = 0.6$ and $z_o/h = 0.1$.

Fetch distance. The largest relative difference in fetch distance exists between configurations B and C, in very unstable conditions and near the canopy top. At $\zeta = -1$, the fetch distances for 90% flux adjustment are $2.73h$ and $2.45h$ at a measurement height of $1.2h$ for configurations B and C, respectively, with a relative difference of only 10%. As z or ζ increases, source configuration becomes even less important. Therefore, for the purpose of deciding fetch criteria in site selection for field campaigns, the exact form of source distribution is not required.

Comparison between Model I and II. In the roughness sublayer, the two models differ most in near-neutral stability: Model II predicts a footprint peak value much lower than the prediction from Model I. For example, at neutral stability, Model II produces a normalized footprint peak value of 0.23 for a measurement height $z/h = 1.2$ whereas Model I gives peak values of 0.46, 0.50 and 0.41 for source configurations A, B, and C, respectively. Thus, the inclusion of the canopy turbulence processes results in a contracted footprint distribution. A random flight simulation that considers the canopy turbulence also produces a contracted footprint distribution over the canopy (Baldocchi, 1997). [On the other hand, the random flight simulation by Rannik et al. (2000) shows that the maxima of footprints from a vertically distributed source shift further upwind and decrease in value, compared to when the atmospheric surface flow is assumed.] In part because of the contraction effect, the vertical flux adjusts more quickly with fetch according

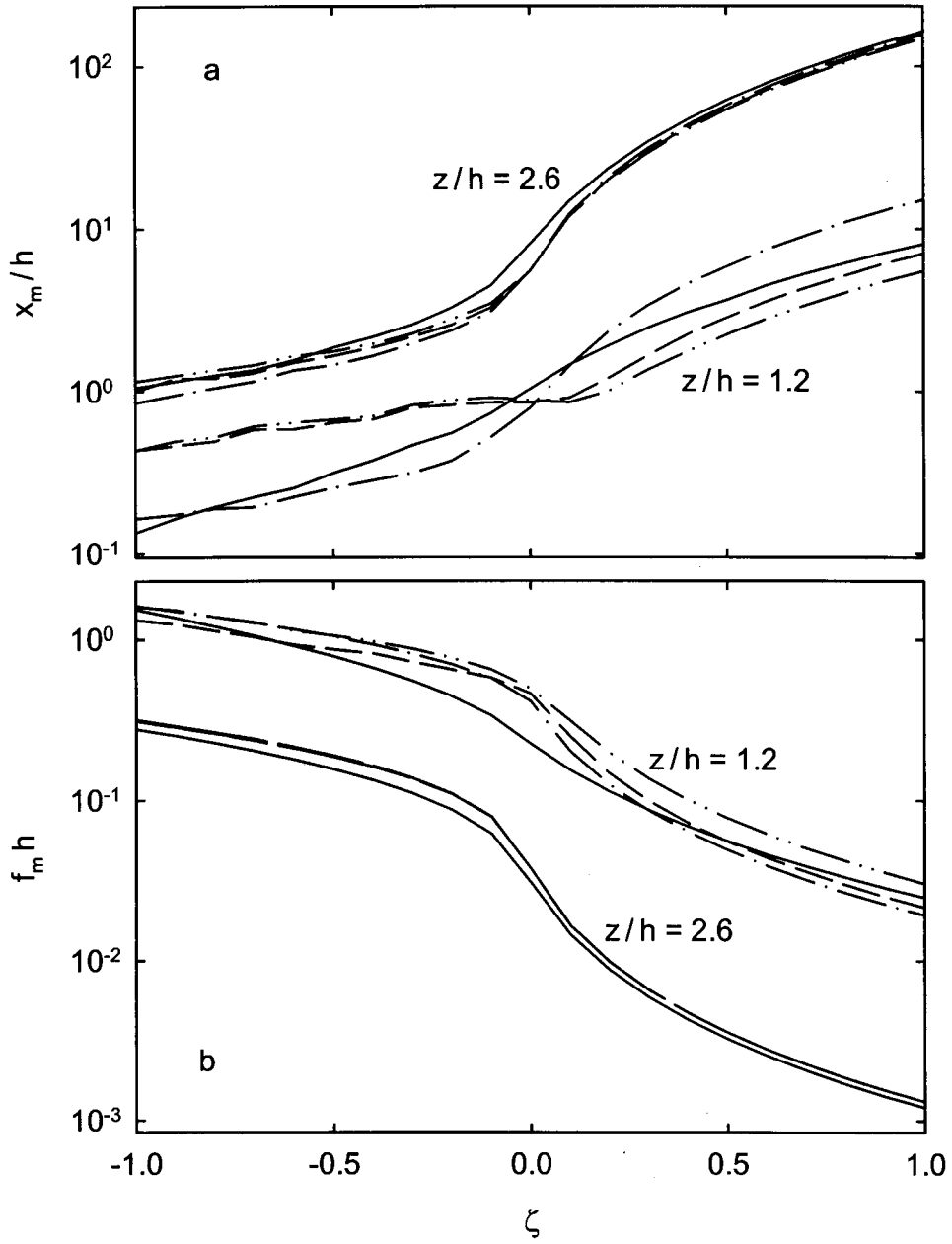

Figure 8. Flux footprint peak position (a) and peak value (b) plotted as a function of air stability for two measurement heights: Dashed line, $F_e/F_T = 0.8$; dash–dot–dot line, $F_e/F_T = 1.2$; dash–dot line, $F_e/F_T = 0.2$; solid line, calculation with Model II using $d/h = 0.6$ and $z_o/h = 0.1$.

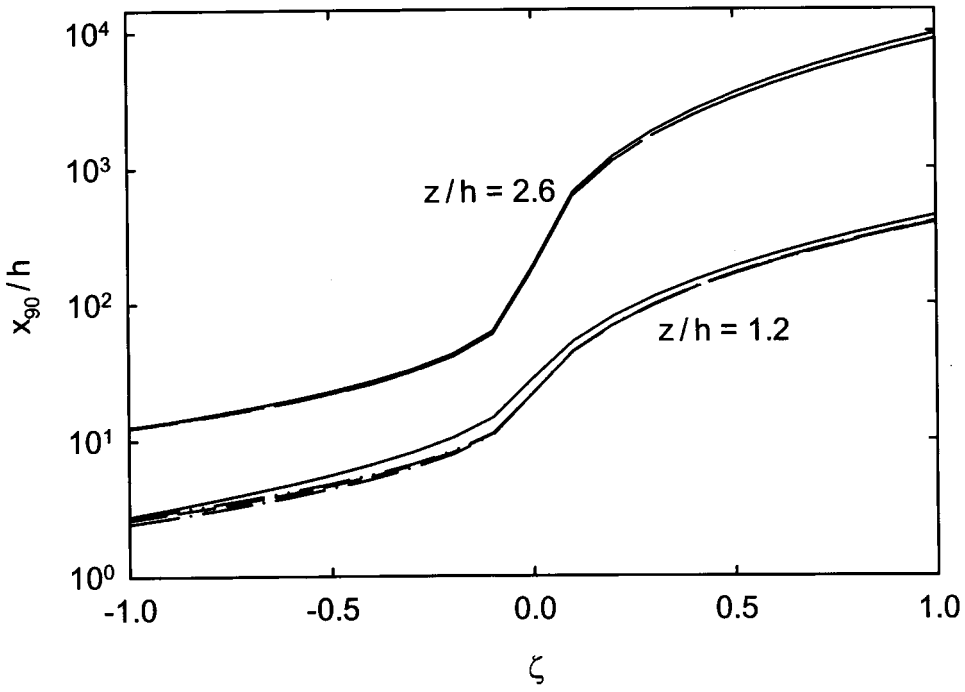

Figure 9. As in Figure 8a but for fetch of 90% flux adjustment.

to Model I, reaching 90% of the NEE at a fetch distance 5–10% closer to the leading edge than the prediction from Model II.

It is also of interest to note that in very unstable conditions, the prediction from Model II resembles the prediction from Model I with source configuration B in which the ground-level source dominates. This is in spite of the fact that Model II effectively places the source at the displacement height. It appears that a large vertical separation between the measurement height and the source height in Model I is compensated by an enhanced eddy diffusion in the roughness sublayer.

In the inertial sublayer, some of the 'contraction effect' remains. Model II predicts that the footprint peaks occur further upwind and decrease in value, compared to predictions from Model I. The fetch distances of 90% flux adjustment are virtually identical.

4.4. Sensitivity analysis

Table I summarizes the calculations of model sensitivity to three key model parameters. The analysis is carried out by changing one parameter by a specific amount and holding others at their default values. The model output is most sensitive to the depth of the roughness sublayer: A 20% change in z_r will result in changes of a similar amount in the 90% fetch distance and the footprint peak value and of a lesser amount in the peak position, noting that an increase in z_r corresponds to a

TABLE I

Model sensitivity to changes in parameter values for height $z/h = 1.6$, neutral stability and source distribution $F_e/F_T = 0.8$. Here x_{90} is fetch distance of 90% flux adjustment, x_m is footprint peak position, and f_m is footprint peak value. The default parameter values are $z_r = 2.16$, $\alpha = 6.5$ and $a_o = 0.2$. Predictions from Model II are given for comparison.

	Model II	Default	z_r		α		a_o	
			+20%	−20%	+20%	−20%	+100%	−100%
x_{90}/h	66	58	54	62	55	63	58	58
x_m/h	2.6	1.6	1.5	1.9	1.4	1.7	1.5	1.7
$f_m h$	0.093	0.17	0.20	0.12	0.18	0.15	0.17	0.15

larger Lagrangian time scale in the roughness sublayer according to Equation (20). The model is insensitive to a_o, indicating that even a crude parameterization of the within-canopy σ_w profile would not cause large uncertainties in the footprint prediction.

The default parameter values are chosen to yield a good match, in terms of the eddy diffusivity enhancement and wind statistics, with the observations made at the Borden forest. In other vegetative stands, the model parameters will vary with canopy morphology and may actually be linked. For example, α usually increases with increasing canopy density. Because the shear layer depth is inversely proportional to α (Raupach et al., 1996), the vertical extent of the influence of shear instability should decrease with increasing canopy density, which in turn may result in a shallower roughness sublayer (Lee, 1997). The effect of the interplay among the parameters is not known, but one could consider the prediction from Model II to be the limit for very dense vegetated surfaces (Table I).

5. Conclusions

The present work extends the published studies on footprint over canopies by combining the LNF theory with parameterizations of the canopy turbulence over a range of stability conditions. The main findings are as follows:

(1) The numerical method for solving the system of equations provides a useful alternative that is free of some constraints inherent in other methods found in the literature.

(2) In the roughness sublayer, the footprint distribution from the LNF prediction is in general more contracted than the prediction based on the inertial sublayer similarity functions. Once in the inertial sublayer, the difference between the two predictions is small, and for practical purposes, solutions derived from the Monin–Obukhov similarity are sufficient.

(3) In unstable conditions, the near-field effect causes the footprint of the elevated canopy source to locate further upwind than the ground-level source and the combined footprint can become negative in situations where the two sources are of opposite sign. In stable conditions, the near-field effect is negligibly small, and the footprint of the ground-level source extends beyond that of the elevated canopy source.
(4) The flux footprint and flux adjustment with fetch in the roughness sublayer are sensitive to source configuration and the parameters specifying wind speed and the Lagrangian time scale inside the canopy. The default parameters values are tuned to various field observations at the Borden forest. It is shown that the parameterization of the Lagrangian time scale as a function of air stability yields eddy diffusivity enhancement in the roughness sublayer that is in reasonably good agreement with the field data.

Acknowledgements

This work was supported by the U. S. National Science Foundation through grant ATM-0072864 and by the Biological and Environmental Research Program (BER), U. S. Department of Energy, through the north-east regional centre of the National Institute for Global Environmental Change (NIGEC) under Cooperative Agreement No. DE-FC03-90ER61010. The author thanks an anonymous reviewer whose comments clarified the meaning of the combined footprint function.

References

Baldocchi, D.: 1997, 'Flux Footprints within and over Forest Canopies', *Boundary-Layer Meteorol.* **85**, 273–292.

Baldocchi, D. and Harley, P. C.: 1995, 'Scaling Carbon Dioxide and Water Vapor Exchange from Leaf to Canopy in a Deciduous Forest. 2. Model Testing and Application', *Plant Cell Environ.* **18**, 1157–1173.

Dyer, A. J.: 1963, 'The Adjustment of Profiles and Eddy Fluxes', *Quart. J. Roy. Meteorol. Soc.* **89**, 276–280.

Horst, T. W. and Weil, J. C.: 1992, 'Footprint Estimation for Scalar Flux Measurements in the Atmospheric Surface-Layer', *Boundary-Layer Meteorol.* **59**, 279–296.

Horst, T. W. and Weil, J. C.: 1994, 'How Far Is Far Enough – The Fetch Requirements for Micrometeorological Measurement of Surface Fluxes', *J. Atmos. Oceanic Tech.* **11**, 1018–1025.

Kaimal, J. C. and Finnigan, J. J.: 1994, *Atmospheric Boundary Layer Flows: Their Structure and Measurement*, Oxford University Press, New York, 289 pp.

Katul, G. G., Leuning, R., Kim, J., Denmead, O. T., Miyata, A., and Harazono, Y.: 2001, 'Estimating CO_2 Source/Sink Distributions within a Rice Canopy Using Higher-Order Closure Model', *Boundary-Layer Meteorol.* **98**, 103–125.

Leclerc, M. Y. and Thurtell, G. W.: 1990, 'Footprint Prediction of Scalar Fluxes Using a Markovian Analysis', *Boundary-Layer Meteorol.* **52**, 247–258.

Leclerc, M. Y., Shen, S. H., and Lamb, B.: 1997, 'Observations and Large-Eddy Simulation of Modeling of Footprints in the Lower Convective Boundary Layer', *J. Geophys. Res.* **102**, 9323–9334.

Lee, X.: 1997, 'Gravity Waves in a Forest: A Linear Analysis', *J. Atmos. Sci.* **54**, 2574–2585.

Lee, X.: 2002, 'Forest-Atmosphere Exchanges in Non-Ideal Conditions: The Role of Horizontal Eddy Flux and its Divergence', in J. Grace et al. (ed.), *Forest at the Land-Atmosphere Interface*, CAB International, in press.

Lee, X., Shaw, R. H., and Black, T. A.: 1994, 'Modelling the Effect of Barometric Pressure Gradient on the Mean Flow within Forests', *Agric. For. Meteorol.* **68**, 201–212.

Leuning, R.: 2000. 'Estimation of Scalar Source/Sink Distributions in Plant Canopies Using Lagrangian Dispersion Analysis: Corrections for Atmospheric Stability and Comparison with a Multilayer Canopy Model', *Boundary-Layer Meteorol.* **96**, 293–314.

Ohtaki, E.: 1985, 'On the Similarity in Atmospheric Fluctuations of Carbon Dioxide, Water Vapor and Temperature over Vegetated Fields', *Boundary-Layer Meteorol.* **32**, 25–37.

Patankar, S. V.: 1980, *Numerical Heat Transfer and Fluid Flow*, Hemisphere Pub. Corp., Washington, DC, McGraw-Hill, New York, NY, 197 pp.

Philip, J. R.: 1959, 'The Theory of Local Advection: I', *J. Meteorol.* **16**, 535–547.

Rannik, Ü., Aubinet, M., Kurbanmuradov, O., Sabelfeld, K. K., Markkanen, T., and Vesala, T.: 2000, 'Footprint Analysis for Measurements over a Heterogeneous Forest', *Boundary-Layer Meteorol.* **97**, 137–166.

Raupach, M. R.: 1989, 'A Practical Lagrangian Method for Relating Scalar Concentrations to Source Distributions in Vegetation Canopies', *Quart. J. Roy. Meteorol. Soc.* **115**, 609–632.

Raupach, M. R., Coppin, P. A., and Legg, B. J.: 1986, 'Experiments on Scalar Dispersion within a Model Plant Canopy. Part I: The Turbulence Structure', *Boundary-Layer Meteorol.* **35**, 21–52.

Raupach, M. R., Finnigan, J. J., and Brunet, Y.: 1996, 'Coherent Eddies and Turbulence in Vegetation Canopies: The Mixing-Layer Analogy', *Boundary-Layer Meteorol.* **78**, 351–382.

Schmid, H. P.: 2002, 'Footprint Modeling for Vegetation Atmosphere Exchange Studies: A Review and Perspective', *Agric. For. Meteorol.*, in press.

Shaw, R. H., den Hartog, G., and Neumann, H. H.: 1988, 'Influence of Foliar Density and Thermal Stability on Profiles of Reynolds Stress and Turbulence Intensity in a Deciduous Forest', *Boundary-Layer Meteorol.* **45**, 391–409.

Simpson, I. J., Thurtell, G. W., Neumann, H. H., and den Hartog, G.: 1998, 'The Validity of Similarity Theory in the Roughness Sublayer above Forests', *Boundary-Layer Meteorol.* **87**, 69–99.

Warland, J. and G. E. Thurtell: 2000, 'A Lagrangian Solution to the Relationship between a Distributed Source and Concentration Profile', *Boundary-Layer Meteorol.* **96**, 453–471.

Wilson, J. D. and Swaters, G. E.: 1991, 'The Sources Area Influencing a Measurement in the Planetary Boundary-Layer – The Footprint and Distribution of Contact Distance', *Boundary-Layer Meteorol.* **55**, 25–46.